American Mineralogist, Volume 87, pages 154–159, 2002

H positions in leucophoenicite, $Mn_7Si_3O_{12}(OH)_2$: A close relative of the hydrous B phases

MARK D. WELCH,[1,*] WILLIAM G. MARSHALL,[2] NANCY L. ROSS,[3] AND KEVIN S. KNIGHT[2]

[1]Department of Mineralogy, The Natural History Museum, Cromwell Road, London SW7 5BD, U.K.
[2]ISIS Facility, Rutherford Appleton Laboratory, Chilton, Didcot, Oxon OX11 0QX, U.K.
[3]Department of Geological Sciences, Virginia Polytechnic Institute and State University, Blacksburg, Virginia 24061, U.S.A.

ABSTRACT

The proton positions in leucophoenicite, ideally $Mn_7Si_3O_{12}(OH)_2$, have been determined by neutron powder diffraction under ambient conditions on a natural sample from Franklin, New Jersey. Refinement in the $P2_1/a$ space group gave $R_p = 2.0\%$ ($wR_p = 2.1\%$), $\chi^2 = 4.04$ for 110 refined parameters. The two non-equivalent protons form a pair of hydroxyl groups and make hydrogen bonds to the same O7 atom of the Si1 tetrahedron at distances of 1.99(1) and 2.09(1) Å. The H···H distance in leucophoenicite is 2.16(1) Å, which is more than twice the Van der Waal's radius of H (>2 Å) and so no proton positional disorder is expected in leucophoenicite. A comparison of the H environments is made between leucophoenicite and Phase B, Superhydrous B, and Phase A.

INTRODUCTION

Understanding the behavior of hydrogenous components of mantle phases is important for interpreting the crystal chemistry and physical properties (elasticity and rheology) of these phases and the mantle rocks in which they occur. Various dense-hydrous-magnesian silicate (DHMS) phases have been synthesized at high pressure and are thought to be potential storage sites for water in the transition zone. Among these are Phase B, $Mg_{12}{}^{[6]}Si^{[4]}Si_3O_{19}(OH)_2$, Superhydrous B, $Mg_{10}{}^{[6]}Si^{[4]}Si_2O_{14}(OH)_4$, and Phase A, $Mg_7{}^{[4]}Si_2O_8[OH]_6$.

Much insight into the important crystal-chemical features of high-pressure mantle minerals has been gained by looking at suitable analogue phases. Leucophoenicite, ideally $Mn_7Si_3O_{12}(OH)_2$, a low-pressure mineral found in Pb-Cu-Zn ore deposits, is one such analogue. Mackovicky (1995) pointed out that there are strong topological similarities between the structures of leucophoenicite and the DHMS compounds Phase B (Finger et al. 1991) and Superhydrous B (Pacalo and Parise 1992). Most notably, the hydrous sheet of Phase B is the same topologically as the structure of leucophoenicite. Both structures contain the serrated ribbon of [Mg,Mn] octahedra that is also characteristic of olivine and humites. Adjacent ribbons are linked by SiO_4 tetrahedra. The hydrous sheets of Phase B and Superhydrous B are shown in Figure 1 along with their characteristic $SiO_4(OH)_2$ cluster. The hydrous B phases and leucophoenicite have close-packed structures that lead to a well-developed layering of polyhedral sheets; only octahedra and tetrahedra are present. Superhydrous B has a straight, unserrated octahedral ribbon. All three phases share the same unusual H configuration in which the H atoms from two neighboring hydroxyl groups form hydrogen bonds ~2 Å in length to the same O atom of an SiO_4 tetrahedron. A similar hydrogen-bonding arrangement occurs in Phase A (Kagi et al. 2000). The distortions of cation octahedra in leucophoenicite are like those of the hydrous sheet of Phase B. The leucophoenicite structure consists of two polyhedral sheets which, in the centrosymmetric structure (see below), are related by inversion centers. In Phase B there is an alternation of a leucophoenicite-type double sheet of composition $Mg_7Si_3O_{12}(OH)_2$ comprising Mg octahedra and Si tetrahedra, and a single anhydrous sheet of Mg and Si octahedra of composition Mg_5SiO_7 (Finger et al. 1991). Leucophoenicite provides a rare opportunity to study H interactions relevant to the hydrous B phases. Ribbeite (Peacor et al. 1987; Freed et al. 1993), ideally $Mn_5Si_2O_8(OH)_2$, is another member of the leucophoenicite group that also includes jerrygibbsite, ideally $Mn_9Si_4O_{16}(OH)_2$. All three minerals contain an $SiO_4(OH)_2$ group. No Mg-analogues of ribbeite or jerrygibbsite are known as yet. A comparison between the H environments in leucophoenicite and ribbeite is made later.

LEUCOPHOENICITE: THE $P2_1/a$ STRUCTURE

The structure of leucophoenicite, without protons, was determined by Moore (1970) in space group $P2_1/a$ and was shown to be made up of polyhedral sheets stacked along **b** with a repeat distance of 4.9 Å. Centers of symmetry are located at the Mn1 cation, at the midpoint of the O7-O7 tetrahedral edge, and between the two Si2 tetrahedra, giving a hydrous double sheet that is also present in Phase B. In the $P2_1/a$ structure the O7-O7 edge is shared by a pair of SiO_4 tetrahedra (Si1) with half occupancy of each tetrahedron. However, on a local scale only one tetrahedron of the Si1 pair is occupied, and the other is occupied by a pair of H atoms forming O-H bonds to O4 and O5 (Moore 1970). Thus, in the real local structure the O7-O7 inversion centers are absent. The actual positions of the two protons and the details of their associated hydrogen bonding are unknown. As pointed out by Mackovicky (1995), orientational long-range ordering of $SiO_4(OH)_2$ clusters in the hydrous B phases is required to preserve the motif of the octahedral [Mg,Si] layer in these structures. This constraint does not exist

* E-mail: mdw@nhm.ac.uk

0003-004X/02/0001–154$05.00

for leucophoenicite, which lacks an octahedral layer. Thus, intra-sheet and inter-sheet orientational disorder of $SiO_4(OH)_2$ clusters is possible in leucophoenicite, with the result that diffraction indicates a centrosymmetric structure. Hence, refinement in $P2_1/a$ is required.

Leucophoenicite is a low-pressure hydrothermal mineral and yet it has qualitatively the same $SiO_4(OH)_2$ cluster as Phase B and Superhydrous B (Fig. 1) which are, characteristically, high-pressure phases. A structural study of leucophoenicite may, therefore, provide interesting crystal-chemical insights into the structural systematics of H in these three closely related structures. The purpose of the present study was to determine the H positions in leucophoenicite and compare them with those in Phase B and Superhydrous B, which are presumed to be similar and have been approximately located by single-crystal X-ray diffraction (Finger et al. 1991; Pacalo and Parise 1992). We have used neutron powder diffraction to this end. Neutron diffraction is well suited to study of the structural details of H behavior because H is much more visible to neutrons than X-rays (stronger scattering of neutrons by a single proton than of X-rays by a single electron). Provided that the mineral is not H-rich, then it is possible to study H directly without deuteration; this was the case for leucophoenicite. Several recent studies have been made of dense high-pressure magnesium silicates using neutron powder diffraction, including Phase A (Kagi et al. 2000), chondrodite (Lager et al. 2001), and clinohumite (Berry and James 2001). In each case it was possible to locate and successfully refine the proton positions.

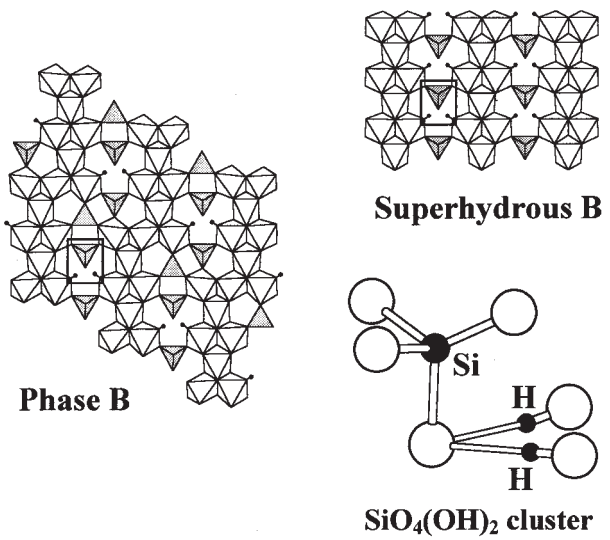

FIGURE 1. The hydrous sheets of Phase B and Superhydrous B showing their common H environment and the different ribbons of octahedral sites and placement of tetrahedra. H atoms are indicated by small solid circles along with their OH bonds. An $SiO_4(OH)_2$ cluster is highlighted in a box for each structure and its bonding topology is also shown in the enlargement (hydrogen bonds are thin rods).

EXPERIMENTAL METHODS

Sample details

A pure sample of leucophoenicite from Franklin, N.J., was used for the study. The specimen from which the experimental sample was taken (BM 1978,518) consists of large prismatic willemite crystals in a matrix of interlocked small, prismatic crystals of pinkish-red leucophoenicite up to 2 mm long. The leucophoenicite crystals fracture easily and could not be extracted intact and not enough material for single-crystal neutron diffraction was available. A total of 2.7 g of leucophoenicite powder was obtained from the hand-specimen for neutron diffraction. Electron microprobe analysis gave an average (n = 10) anhydrous formula $[Mn_{5.92(12)}Mg_{0.16(1)}Ca_{0.64(14)}Zn_{0.22(2)}]_{6.94}Si_{3.03(2)}O_{13}$ (Table 1) that is typical of Franklin leucophoenicites, which always contain Zn and usually Ca as minor elements (Dunn 1985); Fe and F were analyzed for but not detected. High-resolution transmission electron microscopy showed the sample to be exceptionally free of polysomatic defects. Light microscopy showed that the crystals were inclusion-free. There is no evidence chemically or microscopically for the presence of other minerals, including closely related Mn minerals that are often associated with leucophoenicite, e.g., sonolite and jerrygibbsite. Impurity peaks are not evident in the X-ray powder diffraction pattern.

Neutron diffraction

No attempt to deuterate the leucophoenicite sample was made for two reasons: (1) the P-T-f_{O_2} stability of leucophoenicite is unknown and so sample loss would occur in trying to find suitable conditions for H/D exchange, and (2) complete or even a high degree of deuteration is never guaranteed in H/D exchange experiments; moreover, a risk that only partial deuteration is achieved may result in nearly contrast-matched H:D (2:1) values, making H(D) invisible to neutrons.

Ambient powder-diffraction data for the same 2.7 g sample of leucophoenicite were collected using the neutron time-of-flight diffractometers POLARIS and PEARL/HiPr at the ISIS facility, Rutherford-Appleton Laboratory, U.K. POLARIS is a medium-resolution, high-count-rate diffractometer (Smith et al. 1994) with three main detector banks centered at scattering angles $2\theta = 30°$ ($\Delta d/d$ = 1%), 90° (0.7%), and 145° (0.5%). These three large detector banks permit simultaneous data collection over a wide range of d spacings (~0.5–8 Å). PEARL/HiPr is a high-flux, intermediate-resolution diffractometer (ISIS Annual Report 1996), with similar primary and secondary

TABLE 1. Anhydrous formula (O = 13)*

	wt%	cations (apfu)
ZnO	2.52(24)	0.22(2)
MnO	60.5(14)	5.92(12)
CaO	5.20(15)	0.64(14)
MgO	0.95(11)	0.16(1)
SiO2	26.22(32)	3.03(2)
Sum	95.4(6)	9.97(2)

Notes: Standards: Olivine (Mg), wollastonite (Ca, Si), Mn metal, wurtzite (Zn). Values in brackets are one e.s.d. and refer to the last one or two significant figures.
* Average of 10 spot analyses by electron microprobe.

flight-paths to POLARIS. However, it differs considerably from the latter in that the large detector suite is optimized for use with the Paris-Edinburgh pressure cell. This instrument can, nevertheless, be used to collect good quality diffraction data using the principal detector bank centered at $2\theta = 90°$, albeit at a slightly inferior resolution ($\Delta d/d = 0.8\%$) to that of the corresponding bank on POLARIS. The exceptionally high countrate achieved by PEARL/HiPr—typically an order of magnitude greater than POLARIS—is due to the combined effect of the high incident flux from the methane moderator and the large solid angle subtended by the principal detector bank. The total POLARIS and PEARL/HiPr data collection times were equivalent to 400 and 700 μA.h of accumulated ISIS current, respectively. In both experiments, the sample sealed inside a thin-walled vanadium can was set at the reference position of the instrument, that is the sample position for which Lsinθ values had been previously calibrated using a *d*-spacing reference sample (NBS Si powder, SRM640b). For POLARIS, the reproducibility of sample positioning was such that the center of the vanadium can was within 2 mm of the reference position. The corresponding reproducibility for PEARL/HiPr was considerably better (within 0.1 mm), due to the use of a calibrated sample alignment system.

Directly following the POLARIS ambient experiment we collected diffraction data at 13 K so as to "freeze in" the protons. However, the interpretation of the resulting diffraction patterns was complicated by numerous extra peaks arising from magnetic ordering of the Mn ion moments. To date, the details of this new magnetic structure are unknown, but further analysis of these results is in progress. However, it was possible to locate the protons using the ambient data set, and so only the latter is reported here.

Rietveld refinement

Rietveld structure refinement was performed using the program GSAS (Larson and Von Dreele 1994). Data from all three POLARIS detector banks (30°, 90°, 145°) and the single main bank (90°) of PEARL/HiPr were refined simultaneously, the unit-cell parameters being determined from the PEARL/HiPr pattern refinement (see above remarks concerning sample positioning). The $P2_1/a$ structure reported by Moore (1970) was used as a suitable starting model for Rietveld refinement. This model requires that the Si1, H1, and H2 sites are half-occupied, and so their occupancies were fixed at 1/2 throughout the refinement. Based upon crystal-chemical considerations (e.g., Moore 1970), Ca was placed at the Mn2 site, which is the largest of the four octahedra; all other octahedral sites were taken to have the following occupancies, defined by the Mn:Mg:Zn ratios: 0.94Mn + 0.03Mg + 0.03Zn. Similarly, Mn2 = 0.32Ca + 0.64Mn + 0.02Mg + 0.02Zn. The occupancies of all sites were not refined. The following parameter turn-on sequence was used: scale factor, background, peakshape, unit-cell parameters, O *xyz*, O U_{iso}, $^{[6]}$M *xyz*, Si *xyz*, $^{[6]}$M U_{iso}, Si U_{iso}, H *xyz*, H U_{iso}. The displacement parameters of all Mn, both Si and both H atoms were refined together: U_{iso} Mn1 = U_{iso} Mn2 = U_{iso} Mn3 = U_{iso} Mn4, U_{iso} Si1 = U_{iso} Si2, U_{iso} H1 = U_{iso} H2. The starting value of U_{iso} for Mn, Si, and O was 0.01 Å^2, that for H was 0.02 Å^2. Several cycles of least squares were made to refine scale factor, peak-shape, background, and unit-cell parameters before the structural model was refined. The refined unit-cell parameters of leucophoenicite ($P2_1/a$) are a = 10.8259(2) Å, b = 4.8565(1) Å, c = 11.3758(3) Å, b = 103.956(3)°, V = 580.44(2) Å^3, and these values agree well with those of Moore (1970). The protons were located in difference-Fourier maps once satisfactory refinement of all other atoms had been achieved. The experimental, calculated, and difference (observed-calculated) patterns for leucophoenicite are shown in Figure 2.

A problem was encountered in refining the position of the Mn2 cation: improbably large displacements from the octahedral centroid. The origin of this problem lies in the cation composition, $^1/_3$ Ca + $^2/_3$ Mn, which gives a net scattering length of only –0.9 fm, compared with –3.7 fm for the other three Mn cations; the Mn2 cation is therefore almost invisible to neutrons and so its position cannot be refined satisfactorily. To get around this problem, the Mn2 atom coordinates were fixed at the values given by Moore (1970) and the U_{iso} of Mn2 was refined as part of the overall U_{iso} of the four Mn sites.

Refinement based upon F_o^2 proceeded smoothly and converged to an R_p factor of 4.4% without the protons. Both pro-

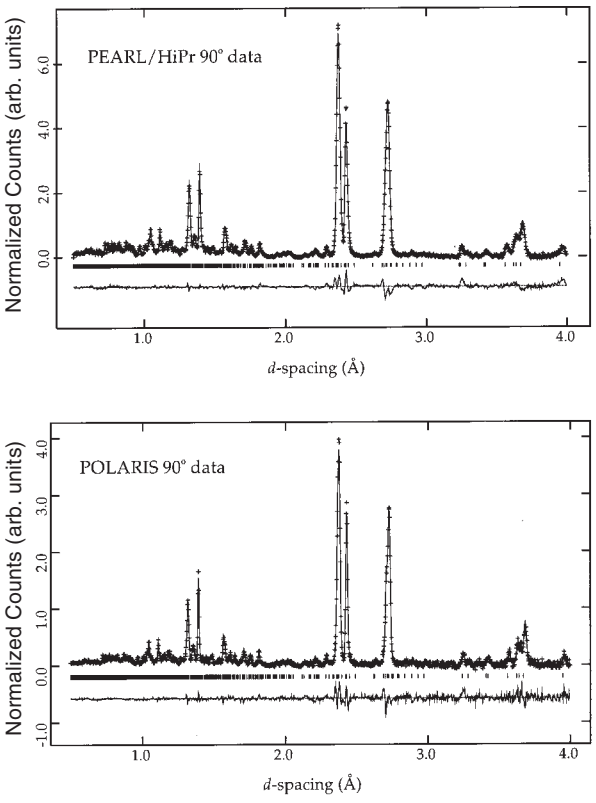

FIGURE 2. Neutron powder diffraction patterns of leucophoenicite for PEARL/HiPr (top) and POLARIS (bottom) data sets for the 90° detector banks. In both patterns data are shown as crosses and the calculated pattern is shown as a continuous line and the difference (observed-calculated) pattern is shown underneath. Reflection markers for leucophoenicite are indicated.

tons were located in difference-Fourier maps and their positions and isotropic displacement parameters were then refined. Their inclusion in the model structure resulted in a final R_p = 2.1% (wR_p = 2.0%) and χ^2 = 4.04 for 110 refined parameters (53 structural, 57 experimental). Both protons are well separated from the fictive Si cation at distances of Si1-H1 = 1.38(1) Å and Si1-H2 = 1.15(1) Å. Atom parameters and selected interatomic distances are given in Tables 2 and 3, respectively. Calculated diffraction patterns for leucophoenicite using the final refined data set with and without protons indicate that the latter contribute ~10% of the diffracted intensity. The intensity ratios of the three intense peaks at 2.4, 2.45, and 2.74 Å are particularly sensitive to H.

DISCUSSION

The final refined atom coordinates and displacement parameters for all atoms (Table 2) are well constrained and agree well with the starting model (Moore 1970). It is noteworthy that the displacement parameters of O4 and O7 are larger than those of the other O atoms, which reproduces the result obtained by Moore (1970). The relatively large displacement parameters of O4 and O7 (and to a lesser degree O5) of the $SiO_4(OH)_2$ cluster may imply dynamic disorder or, perhaps more likely, they reflect the effect of refining an "average" centrosymmetric structure in which two adjacent $SiO_4(OH)_2$ groups are related by the O7-O7 center of symmetry. The unusual character of the T1 site reported by Moore (1970), with its three long and one short Si-O bonds, is also seen in the neutron powder structure. The relative U_{iso} values of the non-H atoms determined here are qualitatively similar to those of Moore (1970). O4 and O7 have the highest U_{iso} values in both studies, followed by O5. These similarities between the two studies lend some credence to the U_{iso} values determined here.

Ribbeite, $Mn_5Si_2O_8(OH)_2$, (Freed et al. 1993) has the same $SiO_4(OH)_2$ cluster as leucophoenicite and the hydrous B phases. It has similar unusual bond lengths as observed for the T1 tetrahedron in leucophoenicite. As with leucophoenicite in space group $P2_1/a$, the space group of ribbeite (*Pnma*) averages the Si occupancy of the edge-sharing T1 tetrahedra (0.5Si) and the associated hydrogens (0.5H1 + 0.5H2). A comparison with ribbeite is given in the next section.

TABLE 2. Atom coordinates and isotropic thermal parameters (Å²)

	x	*y*	*z*	U_{iso}
Mn1	0	0	0	0.0134(4)
Mn2*	0.3149	0.015	0.1396	0.0134(4)
Mn3	0.3308(5)	0.496(1)	0.4157(5)	0.0134(4)
Mn4	0.0870(6)	–0.009(2)	0.2957(6)	0.0134(4)
T1	0.0209(9)	0.423(2)	0.4366(8)	0.0052(4)
Si2	0.1271(4)	0.5753(9)	0.1418(5)	0.0052(4)
O1	0.4916(3)	–0.2174(8)	0.1463(4)	0.0094(7)
O2	0.3398(4)	0.2198(8)	–0.0238(4)	0.0141(8)
O3	0.2270(3)	–0.2901(7)	0.2595(3)	0.0055(6)
O4	0.4151(4)	0.241(1)	0.3041(4)	0.022(1)
O5	0.1753(4)	0.2539(9)	0.4381(4)	0.0134(8)
O6	0.1271(3)	0.2457(7)	0.1442(4)	0.0079(5)
O7	0.5227(5)	0.758(1)	0.4370(4)	0.026(1)
H1	–0.066(1)	0.421(3)	0.326(1)	0.015(1)
H2	0.1265(9)	0.404(2)	0.436(1)	0.015(1)

Notes:
Space group $P2_1/a$:
a = 10.8259(2) Å, b = 4.8565(1) Å, c = 11.3758(3) Å, β = 103.956(3)°, V = 580.44(2) Å³.

Occupancies: Mn1 = Mn3 = Mn4 = Mn; Mn2 = 0.32Ca + 0.64Mn + 0.02Mg + 0.02Zn; T1 = 0.5Si; H1 = H2 = 0.5H; all other sites are fully occupied by the atoms indicated in the Table.

Coordinates are given in a form that allows direct comparison with Table 4 of Moore (1970). Values in brackets are one esd and refer to the last decimal place.
* Coordinates not refined: fixed at the values given by Moore (1970), see text.

TABLE 3. Selected interatomic distances (Å)

Mn1-O1	2.175(4)	T1-O4*	1.84(1)
Mn1-O2	2.169(4)	T1-O5*	1.86(1)
Mn1-O6	2.218(4)	T1-O7*	1.55(1)
average	2.187	T1-O7*	1.81(1)
		average	1.77
Mn2-O1	2.207(3)		
Mn2-O2	2.181(4)	Si2-O1	1.633(5)
Mn2-O2	2.352(4)	Si2-O2	1.629(6)
Mn2-O3	2.364(4)	Si2-O3	1.641(6)
Mn2-O4	2.215(5)	Si2-O6	1.601(5)
Mn2-O6	2.333(3)	average	1.626
average	2.275		
		O4-H1	0.84(1)
Mn3-O3	2.130(7)	O5-H2	0.90(1)
Mn3-O4	2.130(8)	O7-H1	2.09(1)
Mn3-O5	2.118(7)	O7-H2	1.99(1)
Mn3-O5	2.096(8)		
Mn3-O7	2.358(8)	H1-H2	2.16(1)
Mn3-O7	2.399(7)		
average	2.205	T1-H1*	1.38(1)†
		T1-H1*	2.74(2)
Mn4-O1	2.208(9)	T1-H2*	1.15(1)†
Mn4-O3	2.151(7)	T1-H2*	2.54(2)
Mn4-O4	2.292(8)		
Mn4-O5	2.103(8)	O4-O7	2.88(2)
Mn4-O6	2.248(8)	O5-O7	2.89(2)
Mn4-O7	2.252(9)		
average	2.209	O4-H1-O7	158(1)°
		O5-H2-O7	178(1)°

Notes: Values in brackets are one esd and refer to the last decimal place.
* T1 refers to the half-occupied T1 tetrahedron.
† The shortest H distances to the fictive Si at T1 in the $P2_1/a$ structure.

H ENVIRONMENT AND THE $SiO_4(OH)_2$ CLUSTER

The H environments associated with the $SiO_4(OH)_2$ cluster in leucophoenicite are illustrated in Figure 3 for the centrosymmetric (refined) and real local structures. Key interatomic distances involving the protons are given in Table 4, along with the corresponding distances in Phase B, Superhydrous B, Phase A, and ribbeite. The values for Phase A are from neutron powder-diffraction data, whereas those for the hydrous B phases and ribbeite are from X-ray data. In making a comparison between leucophoenicite and the hydrous B phases it must be borne in mind that O-H bond lengths derived from X-ray diffraction are shorter than the true values due to displacement of the H electron toward the O atom. In this respect only a qualitative comparison between H environments in leucophoenicite and the hydrous B phases can be made here.

Both O-H bonds of leucophoenicite are short at 0.84 and 0.90 Å. Other neutron powder diffraction studies of minerals that have reported short O-H or O-D bonds include Phase A (0.89 Å, Kagi et al. 2000) and the Si-free hydrogarnet katoite (0.906 Å, Lager and Von Dreele 1996). Catti et al. (1995) also report an observed O-H bond-length of 0.92 Å for brucite, which

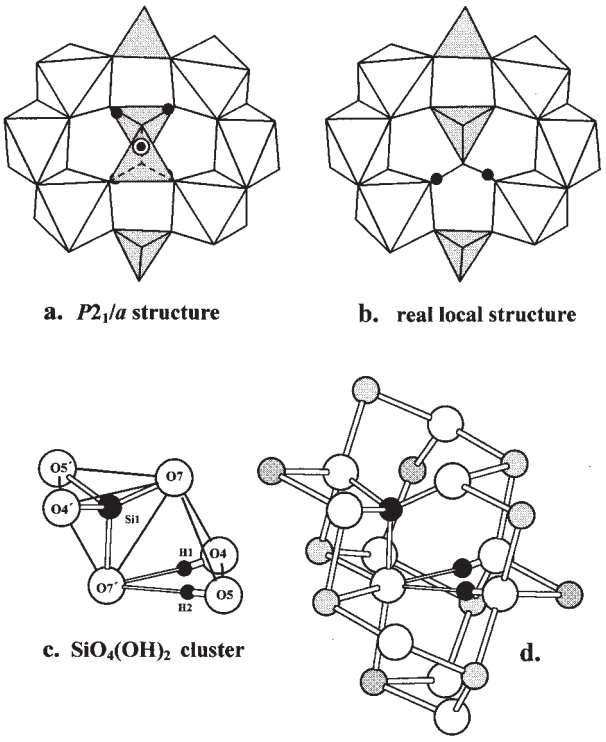

FIGURE 3. The environment of protons in leucophoenicite determined by neutron powder diffraction. (**a**) The $P2_1/a$ structure in which two half-occupied Si1 tetrahedra share a common edge (O7-O7). The inversion center lies midway along the O7-O7 edge and is indicated by a double circle. Protons H1 and H2 are shown as solid circles and two are associated with each Si1 tetrahedron. (**b**) The real structure showing loss of the inversion center, a fully occupied Si1 tetrahedron and two protons H1 and H2. Hydrogen bonds between protons and O7 are shown as lines. (**c**) The $SiO_4(OH)_2$ di-tetrahedral cluster of leucophoenicite with the distinction between O4, O5, O7 and O4', O5', O7' due to loss of the inversion center. Si-O7 is the short tetrahedral bond. The hydroxyl bonds are O4-H1 and O5-H2 and lie near the faces of the "tetrahedron." Hydrogen bonds are shown as thin rods. (**d**) The atomic environment around the T1 tetrahedron in the real structure. Mn sites are gray, Si is the large solid circle, and protons are the two small solid circles. Hydrogen bonds are shown as thin rods as in (**c**).

they correct to 0.96 Å for H riding motion due to positional disorder. Riding motion of H was not reported for katoite or Phase A, despite the short OD bonds. The short O-H bonds in leucophoenicite almost certainly imply some riding motion of H, but this is not reflected in the overall U_{iso} value for H of 0.015 Å^2. Refinement in the $P2_1/a$ average structure leads to larger displacement parameters for some atoms of the $SiO_4(OH)_2$ cluster (O4, O5, and O7) than is really the case. This means that the U_{iso} values for O4 (0.022 Å^2) and O5 (0.013 Å^2) determined for leucophoenicite are unsuitable for applying a riding-motion correction, i.e., U_{iso}(H) is smaller than the U_{iso}(O4) and very similar to U_{iso}(O5). Improved constraints upon H displacement parameters in leucophoenicite could be achieved by deuteration, were this possible.

As in the hydrous B phases, the hydrogen-bond lengths in leucophoenicite (1.99 and 2.09 Å) are similar to each other. The O4-O7 and O5-O7 distances in leucophoenicite are almost equal (2.88 and 2.89 Å), and are very similar to the O-O distances of the hydrous B phases. However, in ribbeite the corresponding distances are both 2.77 Å. Leucophoenicite and Phase A have one straight and one bent O-H····O bond angle, whereas the corresponding bond angles in the hydrous B phases are almost straight. Ribbeite is exceptional in having two very distorted O-H····O bond angles and it also has very short O-H bonds (0.76 and 0.85 Å by X-ray diffraction).

TABLE 4. H distances (Å) and angles (°) in leucophoenicite, ribbeite, the hydrous B phases and Phase A

	Leucophoenicite	Ribbeite[a]	Phase B[b]	Superhydrous B[c]	Phase A[d]
O-H	0.84(1)	0.76(8)	0.82(5)	0.89(2)	0.89(1)
	0.90(1)	0.85*	0.93(6)	–	0.96(1)
H····O	1.99(1)	2.04*	1.96(6)	1.95(2)	1.96(1)
	2.09(1)	2.19(8)	2.03(5)	–	2.29(2)
H····H	2.16(1)	2.68*	1.93(6)	1.89(2)	2.09(1)
			1.86(2)†	1.83(3)†	
O····O	2.88(2)	2.770(3)	2.852(4)	2.83(?)	2.91(2)
	2.89(2)	2.770(3)	2.882(3)	–	3.18(2)
∠O-H····O	158(1)	126(7)	172(5)	179(?)	168(1)
	178(1)	161*	173(5)	–	176(2)

Notes: Values in brackets are one e.s.d. and refer to the last significant figure. a = Freed et al. (1993); b = Finger et al. (1991); c = Pacalo and Parise (1992); d = Kagi et al. (2000).
* H position located in difference-Fourier synthesis but not refined.
† Value determined by ^{1}H NMR spectrocopy by Phillips et al. (1997).

A recent study of leucophoenicite and ribbeite by infrared spectroscopy (Welch et al. in preparation) shows that the room-temperature spectrum of leucophoenicite has two intense broad peaks in the OH-stretching region at 3285 and 3345 cm^{-1}. On the basis of O-H and H····O bond lengths these peaks are assigned to O5-H2 and O4-H1, respectively. As pointed out by Libowitzky (1999), complete substitution of Mg by transition element ions such as Mn^{2+} and Fe^{2+} shifts ν_{OH} by around –50 cm^{-1}. Adding 50 cm^{-1} to the ν_{OH} values observed for leucophoenicite gives 3335 and 3395 cm^{-1}, both in good agreement with those values obtained by Cynn et al. (1996) for Phase B (3351 and 3410 cm^{-1}) and Superhydrous B (3348 and 3404 cm^{-1}). We note that while there is good agreement between the ν_{OH} values of leucophoenicite and the hydrous B phases, these values are lower (by up to 150 cm^{-1}) than the values calculated from the correlations between ν_{OH} and d(O-O) reported by Libowitzky (1999). It seems more likely that this discrepancy reflects deficiencies in the correlations rather than in the structural data of the three phases.

Table 4 shows that the H····H distances in the hydrous B phases are less than twice the Van der Waal's radius of H (<2 Å). An ^{1}H NMR study of the hydrous B phases (Phillips et al. 1997) confirmed that the H····H distances in these two phases are indeed short at 1.86(3) Å in Phase B and 1.83(2) Å in Superhydrous B. Such short H····H distances, being significantly below 2 Å, imply dynamic positional disorder of H. Unfortunately, an ^{1}H NMR study of leucophoenicite is not possible because of the presence of an abundant paramagnetic species (Mn^{2+}). The H····H separation in leucophoenicite is 2.16(1) Å and is similar to that in Phase A of 2.09(1) Å determined by neutron powder diffraction (Kagi et al. 2000). These distances

are more than twice the Van der Waal's radius of H and so, unlike the hydrous B phases, leucophoenicite and Phase A are not expected to have H disorder.

Do the different H····H separations in leucophoenicite and the hydrous B phases relate to the distances between the protons and the nearby cations? The shortest Mn/Mg-H distances in the three phases are similar (2.23–2.27 Å), whereas the Si-H distance in leucophoenicite (2.74 Å) is a little longer than those in Phase B (2.65 and 2.71 Å) and that in Superhydrous B (2.63 Å). Small differences in Si-H coulombic repulsions may be responsible for the different H····H separations of leucophoenicite and the hydrous B phases.

An interesting question arises as to the effects of high pressure upon the hydroxyl bonding arrangement, particularly the H····H separation, in phases having the $SiO_4(OH)_2$ cluster: does pressure shorten the H····H distance and lead to proton disorder? We are currently undertaking a study of leucophoenicite by neutron powder diffraction to explore this possibility.

ACKNOWLEDGMENTS

M.D.W. and N.L.R. gratefully acknowledge support for this work by the Natural Environment Research Council of Great Britain and Northern Ireland (NERC grant GR9/4534). We thank George Lager and an anonymous referee for their constructive comments.

REFERENCES CITED

Berry, A.J. and James, M. (2001) Refinement of hydrogen positions in synthetic hydroxyl-clinohumite by powder neutron diffraction. American Mineralogist, 86, 181–184.

Catti, M., Ferraris, G., Hull, S., and Pavese, A. (1995) Static compression and H disorder in brucite, Mg(OH)2, to 11 GPa: a powder neutron diffraction study. Physics and Chemistry of Minerals, 22, 200–206.

Cynn, H., Hofmeister, A.M., Burnley, P.C., and Navrotsky, A. (1996) Thermodynamic properties and hydrogen speciation from vibrational spectra of dense hydrous magnesium silicates. Physics and Chemistry of Minerals, 23, 361–376.

Dunn, P.J. (1985) Manganese humites and leucophoenicites from Franklin and Sterling Hill, New Jersey: parageneses, compositions, and implications for solid solution limits. American Mineralogist, 70, 379–387.

Finger, L.W., Hazen, R.M., and Prewitt, C.T. (1991) Crystal structures of $Mg_{12}Si_4O_{19}(OH)_2$ (phase B) and $Mg_{14}Si_5O_{24}$ (phase AnhB). American Mineralogist, 76, 1–7.

Freed, R.L., Rouse, R.C., and Peacor, D.L. (1993) Ribbeite, a second example of edge-sharing silicate tetrahedra in the leucophoenicite group. American Mineralogist, 78, 190–194.

ISIS Annual Report (1996) ISSN 1358-6254, 61.

Kagi, H., Parise, J.B., Cho, H., Rossman, G.R., and Loveday, J.S. (2000) Hydrogen bonding interactions in phase A [$Mg_7Si_2O_8(OH)_6$] at ambient and high pressure. Physics and Chemistry of Minerals, 27, 225–233.

Lager, G.A. and Von Dreele, R.B. (1996) Neutron powder diffraction study of hydrogarnet to 9.0 GPa. American Mineralogist, 81, 1097–1104.

Lager, G.A., Ulmer, P., Miletich, R., and Marshall, W.G. (2001) O–D····O bond geometry in OD-chondrodite. American Mineralogist, 86, 176–180.

Larson, A.C. and Von Dreele, R.B. (1994) GSAS general structure analysis system. LAUR 86–748. Los Alamos National Laboratory, New Mexico.

Libowitzky, E. (1999) Correlation of O-H stretching frequencies and O-H····O hydrogen bond lengths in minerals. Monatschefte für Chemie, 130, 1047–1059.

Mackovicky, E. (1995) Structural parallels between the high-pressure B phases and the leucophoenicite series. American Mineralogist, 80, 676–679.

Moore, P.B. (1970) Edge-sharing silicate tetrahedra in the crystal structure of leucophoenicite. American Mineralogist, 55, 1146–1166.

Pacalo, R.E.G. and Parise, J.B. (1992) Crystal structure of superhydrous B, a hydrous magnesium silicate synthesized at 1400 °C and 20 GPa. American Mineralogist, 77, 681–684.

Peacor, D.R., Dunn, P.J., Su, S-C., and Innes, J. (1987) Ribbeite, a polymorph of alleghanyite and member of the leucophoenicite group from the Kombat mine, Namibia. American Mineralogist, 72, 213–216

Phillips, B.L., Burnley, P.C., Worminghaus, K., and Navrotsky, A. (1997) ^{29}Si and ^{1}H NMR spectroscopy of high-pressure hydrous magnesium silicates. Physics and Chemistry of Minerals, 24, 179–190.

Smith, R.I., Hull, S., and Armstrong, A.R. (1994).T he POLARIS Powder Diffractometer at ISIS. Materials Science Forum, 166–169, 251–256.

MANUSCRIPT RECEIVED FEBRUARY 19, 2001
MANUSCRIPT ACCEPTED SEPTEMBER 21, 2001
MANUSCRIPT HANDLED BY BRYAN CHAKOUMAKOS